International Journal of Coal Science & Technology (2022) 9:61
https://doi.org/10.1007/s40789-022-00532-x

RESEARCH

Water-immersion softening mechanism of coal rock mass based on split Hopkinson pressure bar experiment

Zhiyuan Liu[1,3] · Gang Wang[2,3] · Jinzhou Li[1,3] · Huaixing Li[3] · Haifeng Zhao[1] · Hongwei Shi[1] · Jianli Lan[1]

Received: 12 October 2021 / Accepted: 28 June 2022

Abstract

The coal mining process is affected by various water sources such as groundwater and coal seam water injection. Understanding the dynamic mechanical parameters of water-immersed coal is helpful for coalmine safe production. The impact compression tests were performed on coal with different moisture contents by using the ϕ50 mm Split Hopkinson Pressure Bar (SHPB) experimental system, and the dynamic characteristics and energy loss laws of water-immersed coal with different compositions and water contents were analyzed. Through analysis and discussion, it is found that: (1) When the moisture content of the coal sample is 0%, 30%, 60%, the stress, strain rate and energy first increase and then decrease with time. (2) When the moisture content of the coal sample increases from 30% to 60%, the stress "plateau" of the coal sample becomes more obvious, resulting in an increase in the compressive stress stage and a decrease in the expansion stress stage. (3) The increase of moisture content of the coal sample will affect its impact deformation and failure mode. When the moisture content is 60%, the incident rod end and the transmission rod end of the coal sample will have obvious compression failure, and the middle part of the coal sample will also experience expansion and deformation. (4) The coal composition ratio suitable for the coal immersion softening impact experiment is optimized.

Keywords Coal immersion softening · Dynamic compressive response · Split Hopkinson pressure bar · Softening mechanism model

1 Introduction

With the development of coal mining industry, the depth of coal mining continues to increase, and the dynamic disasters in coal mines are increasingly serious (Fan et al. 2019). Understanding the dynamic mechanical parameters of coal rock is of great significance for preventing and reducing the occurrence of disasters (Lin and Zhou 1986). Coal is a porous, inhomogeneous and discontinuous medium composed of multiple mineral components. When the underground water level in the mining area rises, the coal is immersed in the water, and the free water penetrates into the pores and fissures of the coal. This promotes the expansion and connection of pores and fissures, changes the water content and permeability of coal and rock mass, and reduces or even destroys the bearing capacity and strength of coal (Wang et al. 2020; Lama and Bodziony 1998).

In order to develop laboratory coal samples with properties consistent with raw coal under complex geological conditions, a large number of researchers have studied the composition, production process, and mechanical properties of the formed coal samples. Denggao et al. (2005) investigated the influence of coal particle size on briquette through the change of particle size before and after the forming of pulverized coal and the forming of raw materials with different particle sizes, but the influence of moisture on pulverized coal particles during the forming process is not discussed in depth. Xu et al. (2010), Yu et al. (2017) and Wolf and Bruining (2007) pointed out the non-linear relationship

✉ Gang Wang
ckwanggang@163.com

✉ Haifeng Zhao
zhaohf@cup.edu.cn

1 School of Petroleum Engineering, China University of Petroleum, Beijing, Beijing 102249, China

2 Mine Disaster Prevention and Control-Ministry of State Key Laboratory Breeding Base, Shandong University of Science and Technology, Qingdao 266590, China

3 College of Safety and Environmental Engineering, Shandong University of Science and Technology, Qingdao 266590, China

Published online: 21 August 2022

between the strength, permeability, and pore distribution of coal briquette and the composition and particle size of pulverized coal, which provided a more suitable pulverized coal ratio scheme for the study of water-immersion softening of coal. Zhao et al. (2020) studied the effects of moisture ratio, coal particle size, and gas adsorption pressure on isothermal adsorption, and found that moisture could inhibit gas adsorption in coal. Xu et al. (2010) discussed the relationship between pulverized coal particles and pore structure, and pointed out that the smaller the particle size of the briquette, the smaller the pore radius in the briquette. The above-mentioned researchers have studied the influence of the coal body's own components and external factors on its strength, deformation and other characteristics, and have carried out a discussion of the effect of moisture on the coal body's adsorption characteristics. However, further research is needed on coal water-immersion softening.

Therefore, some researchers have studied the influence of moisture on the mechanical properties of coal rock mass (Liu et al. 2021; Kim et al. 2021; Wang et al. 2019). Erguler and Ulusay (2009) quantified the influence of water content on the mechanical properties of rocks and proposed a calculation model for the relationship between moisture content and rock strength. Wang et al. (2018) and Bo-bo et al. (2021) showed that moisture had a significant effect on the deformation of coal samples, and derived a piecewise statistical constitutive model for coal damage considering moisture content. Xiao et al. (2018) established the corresponding relationship between the impact tendency of coal samples with different moisture contents and their acoustic emission signals. Jiang et al. (2016) pointed out that with the increase of the moisture content, the loading and unloading damage of coal samples increased, and the load-bearing strength and residual strength showed a downward trend. Yin et al. (2012), Pan et al. (2010) and Perera et al. (2011) explored the mechanism of the effect of water saturation on the deformation and strength of coal, and found that the water in the coal extended to the tip of the crack through dissolution, thereby promoting crack propagation. Qin et al. (2012) carried out the acoustic emission characteristic test of coal with different moisture contents, and clarified the softening effect of moisture on the mechanical properties of coal (Woo and Kim 2016). Zhang et al. (2020) pointed out that the softening and blocking effects of water made free gas have an inhibitory effect on the deformation of soft coal. Kim and Oliveira (2015) studied the dynamic mechanical properties of sandstone at different water saturations. Those researchers discussed the influence of moisture on the mechanical properties of coal, and established a coal damage model considering moisture content. However, in most of the coal stress methods, steady gradient loading is adopted, and there are few studies on the softening effect of water invasion under dynamic load.

The above researchers mainly studied the influence of coal composition and moisture content on the mechanical properties of coal under low stress loading rate. However, in the actual production activities of coal mining operations, the influence of dynamic factors such as mechanical shock and rock fracture on coal destruction is more complicated (Saleh et al. 2018). Daryadel et al. (2015), Zhu et al. (2009), Mishra et al. (2019), Doner et al. (2019) analyzed the dynamic mechanical properties of the Split Hopkinson Pressure Bar (SHPB) (Roth et al. 2015) on concrete specimens. Ai et al. (2020) studied the crack propagation and dynamic mechanical properties of coal, and found that the bedding direction has a great influence on the dynamic compressive strength, strain rate and strain energy of coal. Yin et al. (2020) tested the strain and energy dissipation characteristics of gas-bearing coal in the SHPB test by changing the gas pressure and static load. Hao et al. (2020) examined the effect of loading rate on the dynamic compressive strength and crack growth of coal samples. Kong et al. (2020, 2021a, 2021b) pointed out that under different confining pressures, gas pressures and impact loads, the failure strength and failure strain of coal samples increased linearly with the strain rate. Zhao et al. (2014) explored the correlation between different bedding directions and dynamic tensile strength, and found that bedding roughness and discontinuity, impact speed, etc. would affect the dynamic mechanical properties of coal. Feng et al. (2020, 2016) reported that the axial fracture of the coal sample was directly caused by the incident compressive stress wave, while the transverse fracture was caused by the reflected tensile stress wave of the coal sample and the transmission rod. Fan et al. (2020), Chengwu et al. (2016) comparatively analyzed the dynamic mechanical characteristics, destruction process and energy dissipation law of explosive coal and anti-explosive coal. Wang et al. (2010) suggested that under impact load, the dynamic strength of saturated sandstone should include the influence of its free water viscosity and Stefan effect. Liu et al. (2012) found that coal rock mainly exhibited axial splitting failure at low strain rate and crush failure at high strain rate. Chengwu et al. (2012) decomposed the measured SHPB test signal of coal impact damage by using the empirical mode decomposition method. Compared with metal and rock specimens, water-soaked coal samples have lower strengths making it more difficult to obtain effective impact data. However, strong dynamic impact specimens commonly exist in underground coalmines, and thus relevant research can be carried out.

In summary, (1) Some researchers have pointed out that there is a nonlinear relationship between the strength of briquette and the particle size of pulverized coal, and that moisture will increase its complexity. (2) Other researchers have studied in detail the effect of moisture on the mechanical properties of coal under low stress loading rate. (3) However,

there is a lack of research on the softening mechanism of coal under high stress loading rate and there are few studies on the damage form of water-flooded coal under impact load although impact load in coalmines is a relatively common dynamic form. Therefore, in order to find a suitable laboratory sample to replace the raw coal specimen wetted by water injection, the impact load of the coal sample is analyzed through the SHPB dynamic impact test in this paper. Starting from the composition and moisture content of the coal sample, the damage characteristics of the coal sample under impact load are analyzed and optimized, which is more in line with the coal seam type and the standard coal-blending scheme based on rock mechanics. This lays the experimental material foundation for revealing the mechanism of coal seam water injection.

2 Design of dynamic mechanical test of water immersed coal

2.1 Split Hopkinson pressure bar test system

As shown in Fig. 1, the SHPB test apparatus includes a pressure bar, ultra-high dynamic strain gauges, an oscilloscope and a data acquisition system. The strut is 50 mm in diameter, and the bullet, strut, and absorption rod are made of the same material. The elastic modulus is 206 MPa, the density is 7850 kg/m^3, the bullet length is 500 mm, the incident and projection rod length is 3000 mm, and the wave velocity is 7143 m/s. The principle of the SHPB test is as follows. At different impact velocities, the punch acts on the incident rod, generating stress waves on the incident rod. After the stress waves contact the sample, reflected waves and incident waves are generated on the incident rod and transmission rod, respectively, and the data acquisition system records the data of the strain gauges on each compression bar.

2.2 Composition ratio of coal sample for immersion experiment

The pulverized coal was taken from the N2808 working face of the No. 8 anthracite coal seam of Yuyang Coal Mine of Chongqing Songzao Coal and Electricity Co., Ltd. The specific parameters of the coal mass are shown in Table 1.

In order to study the relationship between the immersion softening mechanism and mechanical parameters of coal, coal samples with different mechanical properties are prepared by configuring different coal sample components in this paper (Table 2). Cement, sand, activated carbon, and

Table 1 Industrial analysis parameters of pulverized coal

Parameter	Value
Volatile content (%)	9.87–10.97
Ash content (%)	11.53–19.13
Moisture content (%)	0.56–2.55
True density (g/cm^3)	1.50–1.53
Apparent density (g/cm^3)	1.34–1.38
Robustness coefficient	0.21–0.38
Uniaxial peak strength (MPa)	Less than 1
Coal failure type	Class III–V

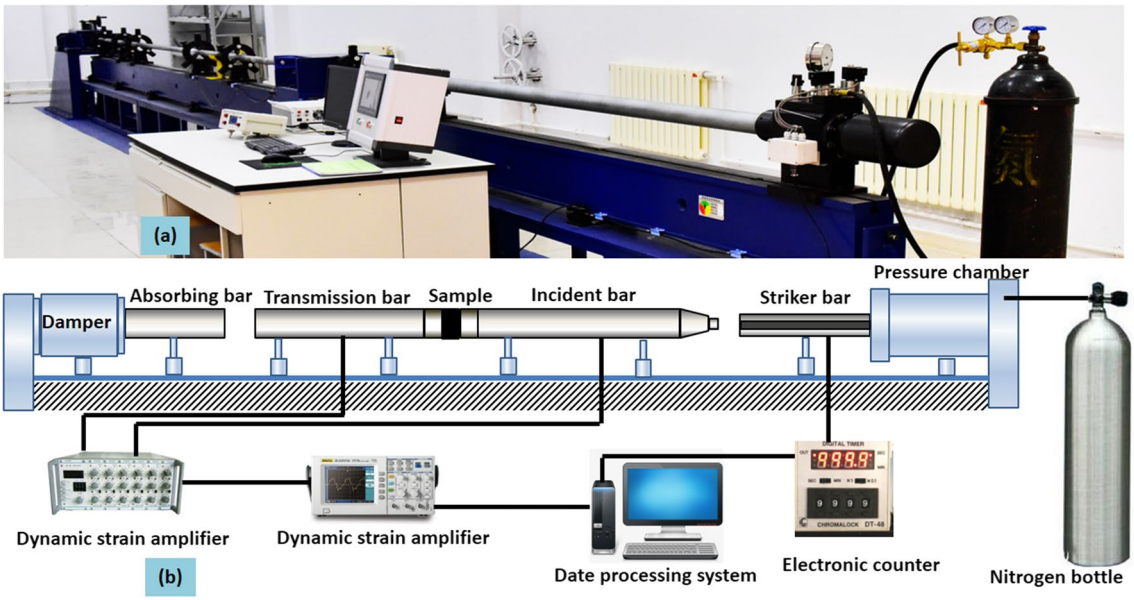

Fig. 1 Split Hopkinson pressure bar test apparatus. **a** Photo of SHPB apparatus; **b** Schematic diagram of SHPB apparatus

Table 2 Composition of prepared coal samples

Composition ratio scheme	Cement (425 ordinary Portland cement)	Sand (ordinary river sand, particle size 20–40 mesh)	Water (pure water)	Activated carbon (granular, Φ2.6 mm × 5.6 mm)	Coal powder (particle size 20–40 mesh, 40–80 mesh, ratio 1:1)
1	4.0	3.5	8.25	0.88	83.37
2	5.0	6.0	7.75	0.7	80.55
3	6.0	2.5	6.50	0.90	84.10
4	7.0	5.5	8.50	0.84	78.16
5	8.0	2.0	7.25	0.78	81.97

coal powder of different particle sizes are used to prepare coal samples with relatively uniform pore and fissure structures compared with that of the raw coal (Doner et al. 2019).

2.3 Preparation of water-immersed coal samples for dynamic mechanics test

In order to study the mechanism of coal immersion softening, and to make the effect of immersion softening more obvious, three immersion schemes with a large gradient are designed: dry coal sample, coal sample with a moisture content of 30% and coal sample with a moisture content of 60%. In order to eliminate the influence of residual moisture in the production process, the coal samples in Sect. 2.1 are first dried, and then the coal samples to be immersed are weighed. During the immersion process, the water does not need to be pressurized, that is, the coal sample is immersed in a water container. According to the moisture absorption capacity of the coal sample, a certain amount of water is absorbed to reach the moisture content required by the experiment. Finally, the soaked coal samples are wrapped in plastic wrap and put into the storage box ready for the SHPB test.

3 Experiment process and result analysis

3.1 Experiment process and results

This test is mainly to study the influence of coal composition and water immersion on the softening mechanism of coal. Therefore, each type of water-bearing coal sample consists of 5 groups of coal samples with different components, and each group of 3 coal samples is subjected to repeated tests. After the SHPB test is conducted on the coal samples with different moisture contents, the stress, strain, and strain rate of the samples are calculated by the "dual wave method" (Larbi et al. 2015). Through data processing, the changes in the stress, strain, strain rate and energy of the coal samples over time are obtained (Al-salloum et al. 2015).

$$\begin{cases} \varepsilon_*(t) = -\frac{2C}{l_0}\varepsilon_{\mathrm{r}}(t) \\ \varepsilon(t) = -\frac{2C}{l_0}\int_0^t \varepsilon_{\mathrm{r}}(t)\mathrm{d}t \\ \sigma(t) = \frac{A}{A_0}E\varepsilon_{\mathrm{r}} \end{cases} \tag{1}$$

where C is the elastic wave velocity, E is the elastic modulus, A is the cross-sectional area of the compression bar, l_0 is the length of the test sample, A_0 is the cross-sectional area of the test sample, ε_{r} is the measured strain from the reflected waves, σ is the measured stress.

Figure 2 shows the stress, strain and energy dissipation of the dry coal sample within 180 us. In this Fig., the stress, strain rate and energy dissipation of the coal sample first increase and then decrease with time while the strain almost always increases. Figure 2a shows the change of coal sample stress with time, where the negative stress is defined as the compressive stress, and the positive stress as the expansion stress. At first, the stress increases with time. After reaching the turning point, it begins to decrease and becomes the failure stress. Figure 2b shows the variation of coal sample strain with time. For the Nos. 3 and 5 coal samples, the strain first increases slowly, then rapidly, and finally slowly. However, this change is not obvious for other coal samples. Figure 2c shows the change of the strain rate of the coal sample with time. Compared with the staged change of stress and strain, the staged change of strain rate is more obvious. However, due to the influence of the coal sample composition, the turning points between the stages are different. Figure 2d shows the temporal variation of the energy dissipation of the coal sample throughout the entire destruction process. Combined with Fig. 2b, it can be seen that the coal sample consumes a lot of energy during the large deformation stage.

Figure 3 shows the stress, strain and energy dissipation of the coal sample with a water content of 30%. Compared with the change rule of the dry coal sample, the characteristic rule of the four parameters of the coal sample is more obvious. From the overall analysis, the effect of coal immersion

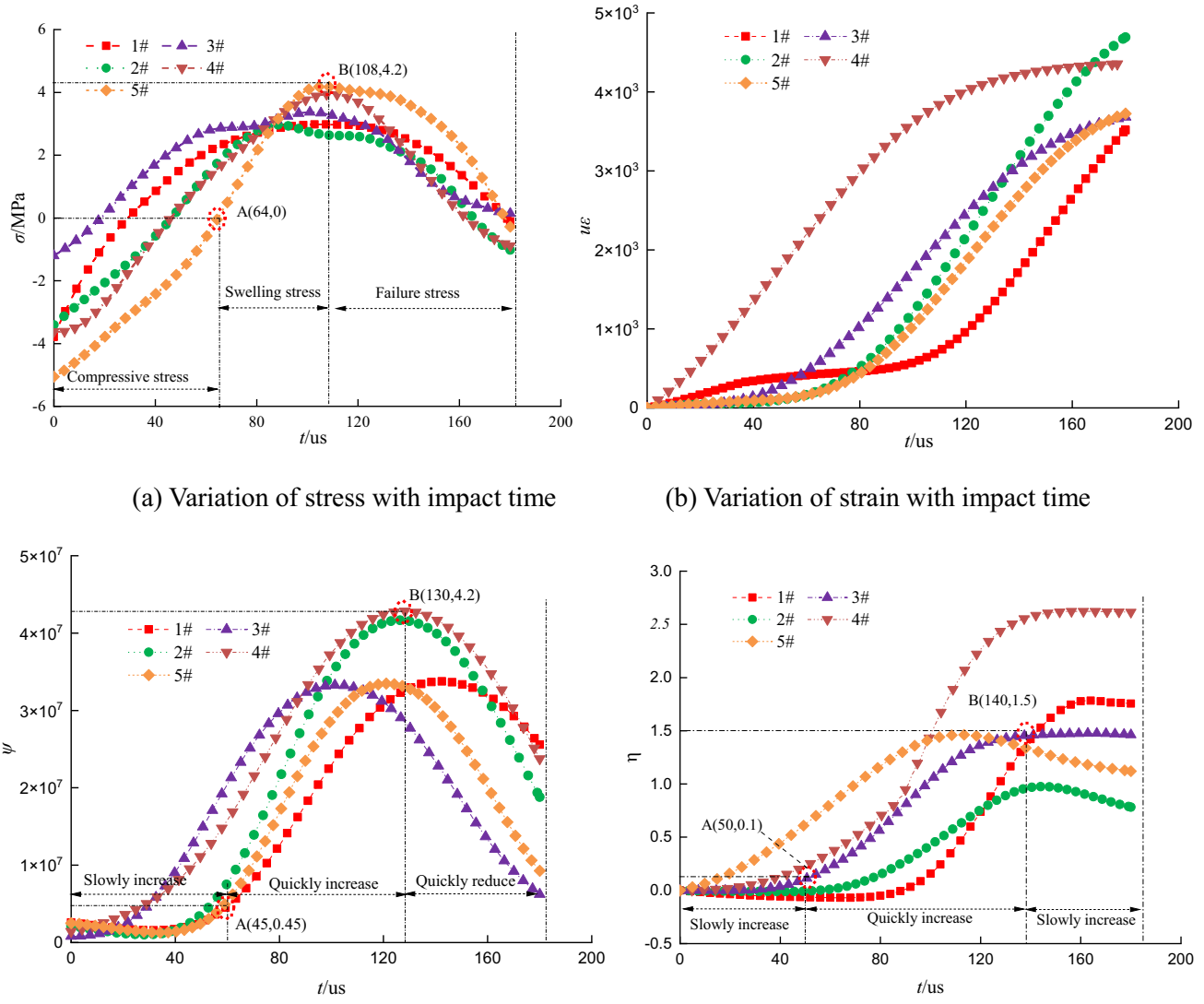

(a) Variation of stress with impact time

(b) Variation of strain with impact time

(c) Variation of strain rate with impact time

(d) Variation of energy dissipation with impact time

Fig. 2 Dynamic mechanical characteristics of coal with a water content of 0%. **a** Variation of stress with impact time; **b** Variation of strain with impact time; **c** Variation of strain rate with impact time; **d** Variation of energy dissipation with impact time

is regular, especially the evolution of the strain of the coal sample over time (Kong et al. 2020). In Fig. 3a, a "plateau" appears for the Nos. 1, 2, and 3 coal samples after the expansion stress is generated in the coal samples, that is, the rate of increase of stress decreases, indicating that the internal moisture of the coal sample has a certain buffer effect on the deformation of the coal samples. Figure 3b shows that the strain of the coal sample has a slow increasing trend before 60 μs owing to the influence of water immersion. After the subsequent rapid growth, the strains of the 5 coal samples with different compositions exhibit a slow increasing trend again (Feng et al. 2020). Figure 3c indicates that the strain rate change curve of the coal sample with a water content of 30% is similar to that of the dry coal sample. The strain rate of the coal sample is in a slow increase stage within the first 45 μs, and then enters a rapid increase stage until 130 μs. Further analysis of the strain rate of the coal sample indicates that the strain rate changes in the slow growth stage, the rapid growth stage and the rapid decline stage are more obvious than those of the dry coal sample. This means that water can promote an increase in the internal deformation of the coal sample. Figure 3d shows the energy dissipation during the entire destruction process of the coal sample. Compared with the energy dissipation of the dry coal sample, the slow growth stage of energy dissipation takes longer. In addition, the rapid growth stages of the No. 5 coal samples with a water content of 30% are relatively regular, indicating that water can activate the coal samples to absorb energy.

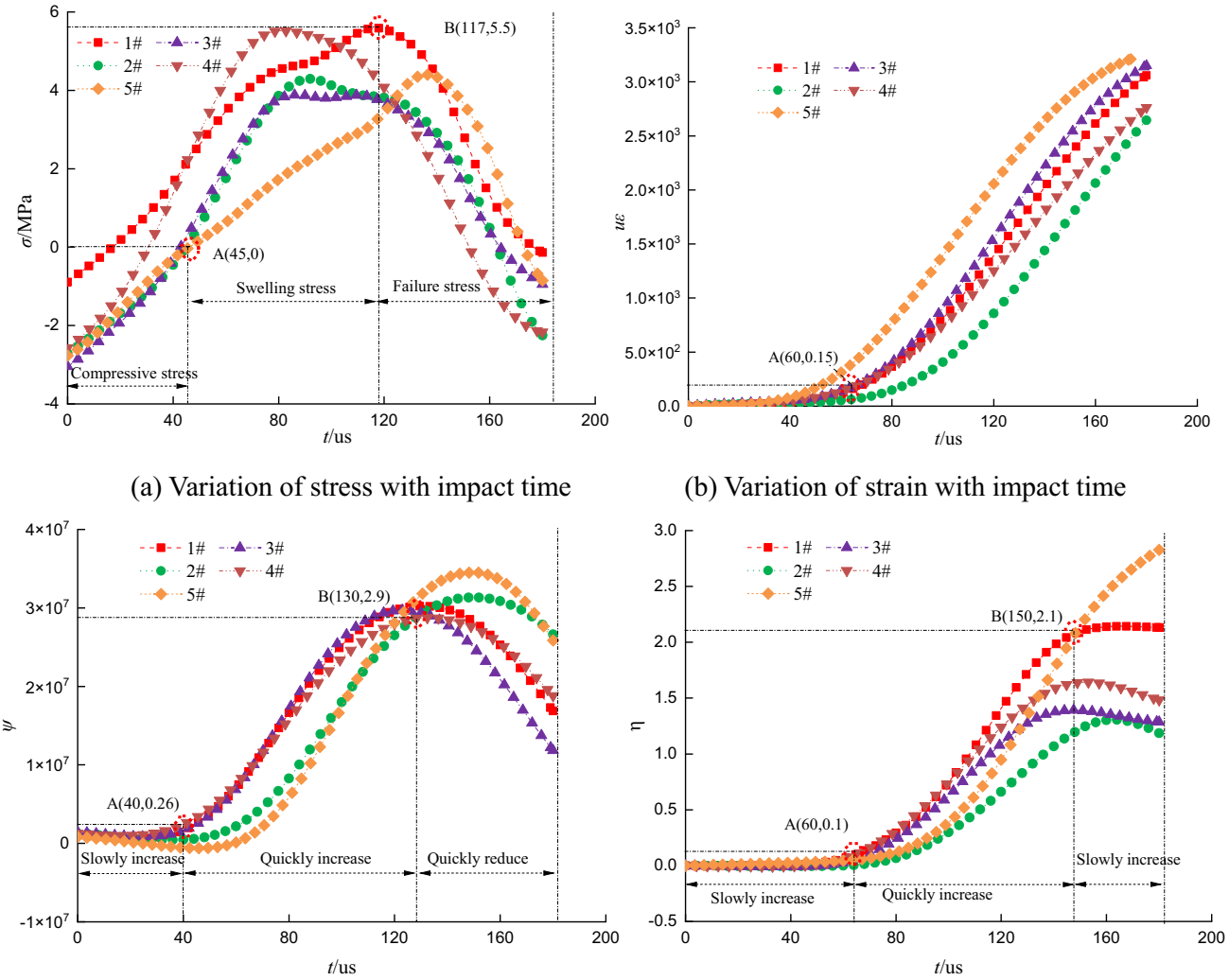

(a) Variation of stress with impact time

(b) Variation of strain with impact time

(c) Variation of strain rate with impact time

(d) Variation of energy dissipation with impact time

Fig. 3 Dynamic mechanical characteristics of coal with a water content of 30%. **a** Variation of stress with impact time; **b** Variation of strain with impact time; **c** Variation of strain rate with impact time; **d** Variation of energy dissipation with impact time

Figure 4 shows the variation of stress, strain and energy dissipation over time when the moisture content of the coal sample increases to 60%. As indicated in Fig. 3a and Fig. 4a, when the water content of the coal sample increases from 30% to 60%, the stress "plateau" of the coal sample disappears, the compressive stress stage becomes longer, and the expansion stress stage becomes shorter. In addition, the failure stress stage is also significantly shortened. By comparison of Figs. 3b and 4b, it is found that with the increase of the water content, the first slow increasing stage of the strain becomes longer, and the rapid increasing stage does not change much, but the second slow increasing stage disappears. Figure 4c shows a more obvious stage variation and the variation patterns of the five coal samples are also more uniform. From the change of strain rate with time alone, the effect of water immersion on the coal samples with a water content of 60% is more obvious than that on the coal samples with a water content of 0% and 30%. Figure 4d shows the energy dissipation curve of coal sample destruction. When the water content increases to 60%, the first slow increasing stage of energy dissipation becomes longer, and the rapid increasing stage and the second slow increasing stage become shorter, indicating that the energy consumed during the destruction process of the coal mass is reduced after the coal mass is immersed in water.

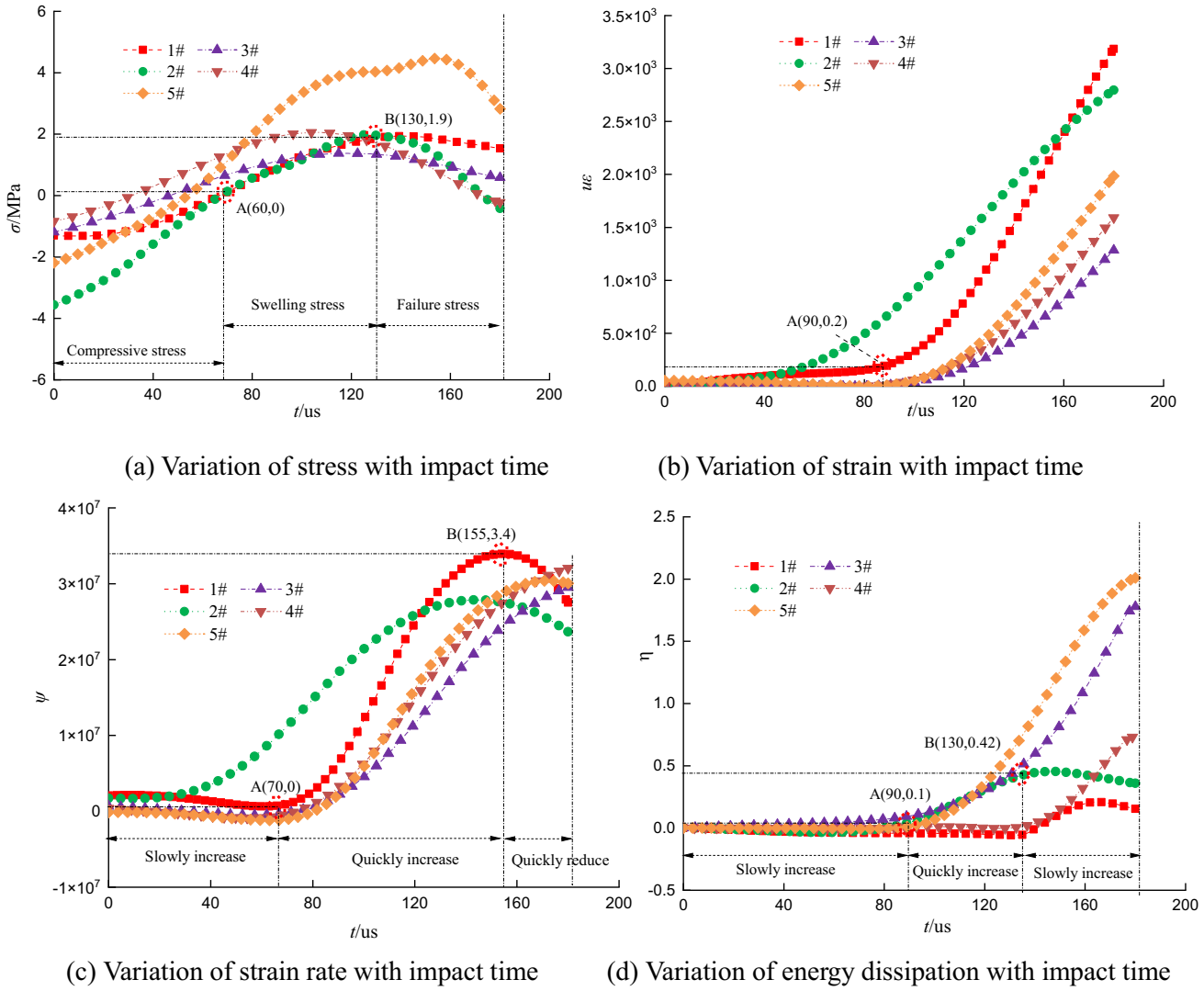

(a) Variation of stress with impact time

(b) Variation of strain with impact time

(c) Variation of strain rate with impact time

(d) Variation of energy dissipation with impact time

Fig. 4 Dynamic mechanical characteristics of coal with a water content of 60%. **a** Variation of stress with impact time; **b** Variation of strain with impact time; **c** Variation of strain rate with impact time; **d** Variation of energy dissipation with impact time

3.2 Analysis of test results

3.2.1 Analysis of immersion softening mechanism of coal mass on microscopic scale

According to classic damage mechanics, the Drucker-Prager failure criterion has the advantages of simple parameter form and wide application in rock materials. When the rock is damaged by a three-dimensional stress, the strength of each component is (Majedi et al. 2021):

$$\begin{cases} I_1 = \sigma_1^* + \sigma_2^* + \sigma_3^* \\ J_2 = \frac{1}{6}\left[\left(\sigma_1^* - \sigma_2^*\right)^2 - \left(\sigma_2^* - \sigma_3^*\right)^2 - \left(\sigma_3^* - \sigma_1^*\right)^2\right] \end{cases} \tag{2}$$

Under the condition of triaxial stress, $\sigma_i^*(i=1, 2, 3)$ (Wang et al. 2018), when there is no fluid inside the rock, the triaxial stress forms an effective stress, and thus the corresponding strain $\varepsilon_i^*(i=1, 2, 3)$ (Jacquelin et al. 2017) is generated. According to Hooke's Law:

$$\varepsilon_1 = \frac{1}{E}\left(\sigma_1^* - \mu\sigma_2^* - \mu\sigma_3^*\right) \tag{3}$$

where μ is the Poisson's ratio of the rock, E is the initial elastic modulus, and ε_1 is the axial strain of the rock.

Then the effective damage stress of the rock is (Butt and Xue 2014):

$$\sigma_1^* = \sigma_i/(1-D), \quad (i=1,2,3) \tag{4}$$

where D is the statistical damage variable.

The statistical damage variable D is defined as follows:

$$D = \frac{N_a}{N} \tag{5}$$

where N is the number of micro-units that the rock can be divided into, and N_a is the number of damaged micro-units in the rock.

Assuming that the micro-units obey the Weibull distribution, the density function of the number of damaged micro-units in the rock is:

$$P(F_1) = \frac{m}{F_0}\left(\frac{F_1}{F_0}\right)e^{\left[-\left(\frac{F_1}{F_0}\right)^m\right]} \tag{6}$$

where F_0 and m are the Weibull distribution parameters, and F_1 is the strength variable of the rock micro-unit at the first failure point.

Then the damage of dF_1 extends to the inside of the rock. At this time, the failure interval of the rock is (F_1, F_1+dF_1), and the number of damaged micro-units inside the rock is $NP(x)$, that is, the total number of damaged micro-units in the stressed rock is:

$$N(F) = \int_0^{F_1} NP(x)dx = N\left\{1 - \exp\left[-\left(\frac{F_1}{F_0}\right)^m\right]\right\} \tag{7}$$

After Eq. (7) is substituted into Eq. (6), the damage variable D of the rock can be obtained (Ai et al. 2020):

$$D = 1 - \exp\left[-\left(\frac{F}{F_0}\right)^m\right] \tag{8}$$

Therefore, by substituting Eq. (4) into Eq. (3), we can obtain:

$$\varepsilon_1 = \frac{\sigma_1 - \mu\sigma_2 - \mu\sigma_3}{E(1-D)} \tag{9}$$

Combining Eq. (9) and Eq. (4), we get:

$$\sigma_1^* = \frac{\sigma_i E\varepsilon_1}{\sigma_1 - \mu\sigma_2 - \mu\sigma_3}, (i = 1, 2, 3) \tag{10}$$

When the coal mass is immersed in water, the water moves in the fissure structure of the coal mass in the form of laminar flow, and performs capillary or diffusion movement in the smaller pores. Therefore, capillary force or self-suction force is introduced into the water-immersed coal mass. Assuming that water produces capillary force inside the pores of the coal sample and surface tension on the surface of the water, the force of water will exist in the form of "liquid bridge force". This means that when moisture condenses in the pores between the pulverized coal particles, the moisture and the particles form a common micro-unit force body. With more and more water in the pores, the thickness of the water film between the particles increases, and the resulting liquid bridge force also increases, thereby increasing the cohesive force between the pulverized coal particles. However, there is a certain upper limit for the self-suction of the pores. When the water film increases to a certain thickness, the change in this cohesive force decreases. From a microscopic point of view, there are many influencing factors, such as the viscosity coefficient of the liquid and the distance between the pulverized coal particles. In the case of an infinitesimal body, the liquid bridge force inside the infinitesimal body is simplified to:

$$\sigma_w = \sigma_{w1} + \sigma_{w2} \tag{11}$$

where σ_w is the liquid bridge force in the micro-unit body, σ_{w1} is the static liquid bridge force in the micro-unit body, and σ_{w2} is the dynamic liquid bridge force in the micro-unit body.

The expressions of the two liquid bridge forces are (Bariani et al. 2011):

$$\begin{cases} \sigma_{w1} = 2\pi\varphi - \pi\varphi^2\gamma\left(\frac{1}{\varphi} + \frac{1}{\omega}\right) \\ \sigma_{w2} = \frac{3}{2}\pi\epsilon R\upsilon \end{cases} \tag{12}$$

where φ is the distance between the pulverized coal particles, ω is the contact angle between the pulverized coal particles and water, and υ is the viscosity coefficient of water.

The dimensionless tension parameter C_a is usually used to measure the ratio of the dynamic liquid bridge force to the static liquid bridge force:

$$C_a = \frac{\mu_l \cdot v_r}{\gamma} \tag{13}$$

Assuming that the temperature is 20 ℃. At this temperature, the surface tension coefficient γ of water is 0.07275 N/m, the viscosity coefficient μ_l is 1.01×10^3 N s/m^2, and the maximum value of the relative velocity between particles v_r is 2.084 m/s. In this paper, only the capillary force, i.e., the static liquid bridge force, is considered in the calculation of the liquid bridge force. Therefore, assuming that the adhesion force between pulverized coal particles and water is the liquid bridge force, the calculation equation is:

$$\frac{\sigma_w}{a} = 2\pi\sigma_\gamma\cos\theta_p \tag{14}$$

where σ_γ is the surface tension of water, and θ_p is the contact angle between coal particles and water.

The calculation equation of the liquid bridge force is further transformed into:

$$\frac{\sigma_w}{a} = \frac{2\pi\sigma_\gamma\cos\theta_p}{(1 + H/2d)} \tag{15}$$

where a is the radius of the pulverized coal particle, H is the length of the liquid bridge or the distance between two pulverized coal particles, and d is the immersion height of

the liquid bridge or the height of the pulverized coal particle that can be wrapped by water to remove the surface tension.

3.2.2 Analysis of macroscopic strength failure based on microscopic coal immersion softening

Combined with the strength analysis of the rock micro-unit body, the macro-strength criterion of the unimmersed coal sample is derived as follows. Using the Lemaitre equivalent strain principle, we obtain:

$$\sigma = E\varepsilon_1(1-D) + \mu(\sigma_2+\sigma_3) \tag{16}$$

Substituting Eq. (8) into Eq. (16), we get (Merle and Zhao 2006):

$$\sigma = E\varepsilon_1 p\left[-\left(\frac{F_1}{F_0}\right)^m\right] + \mu(\sigma_2+\sigma_3) \tag{17}$$

After further substituting into Eq. (2) and simplifying, we have (Tuazon et al. 2014):

$$\begin{cases} I_1 = \frac{\sigma_1+\sigma_2+\sigma_3}{\sigma_1-\mu\sigma_2-\mu\sigma_3} \\ J_2 = \frac{1}{6}\left[\left(\frac{\sigma_1-\sigma_2}{1-D}\right)^2 + \left(\frac{\sigma_2-\sigma_3}{1-D}\right)^2 + \left(\frac{\sigma_3-\sigma_1}{1-D}\right)^2\right] \end{cases} \tag{18}$$

It is assumed that $\sigma_2=\sigma_3=0$, that is, the coal sample is subjected to uniaxial stress. At this time, without considering the influence of water, we obtain the strength damage model of the coal sample (Al-salloum et al. 2015):

$$\begin{cases} \sigma = E\varepsilon_1 p\left[-\left(\frac{F_1}{F_0}\right)^m\right] \\ I_1 = E\varepsilon_1 \\ J_2 = \frac{1}{6}(E\varepsilon_1)^2 \end{cases} \tag{19}$$

When the immersed coal sample is under uniaxial compression, its strength damage model is:

$$\begin{cases} \sigma = E\varepsilon_1 p\left[-\left(\frac{F_1}{F_0}\right)^m\right] + \mu\sigma_w \\ I_1 = \frac{\sigma_1+\mu\sigma_w}{\sigma_1-\mu\sigma_w} \\ J_2 = \frac{1}{6}\left[(E\varepsilon_1)^2\right] \end{cases} \tag{20}$$

It can also be expressed as:

$$\begin{cases} \sigma = E\varepsilon_1 p\left[-\left(\frac{F_1}{F_0}\right)^m\right] + 2\pi\mu a\frac{\sigma_\gamma\cos\theta_p}{(1+H/2d)} \\ I_1 = 1 + \frac{4\pi\mu a\sigma_\gamma\cos\theta_p}{\sigma_1(1+H/2d)-2\pi\mu a\sigma_\gamma\cos\theta_p} \\ J_2 = \frac{1}{6}\left[(E\varepsilon_1)^2\right] \end{cases} \tag{21}$$

Figure 5 shows the transformation relationship between compressive stress, expansion stress and failure stress of the coal samples with different water contents. When the water content of the coal sample increases from 0% to 60%, the failure stress stage of the five coal samples decreases while the expansion stress stage increases. However, there is no uniform relationship between changes in the compressive stress stage. This means that after the coal sample is immersed in water, the water inside the coal sample helps to increase the expansion stress stage of the coal sample. For the Nos. 2 and 5 coal samples, the above-mentioned change characteristics are particularly obvious. From the analysis of coal sample composition, in the No.2 coal sample the proportion of activated carbon is 0.7% and the proportion of pulverized coal is 80.55%, while in the No.5 coal sample the proportion of activated carbon is 0.78% and the proportion of pulverized coal is 81.97%. The two compositions of the two coal samples are similar to those of the other coal samples.

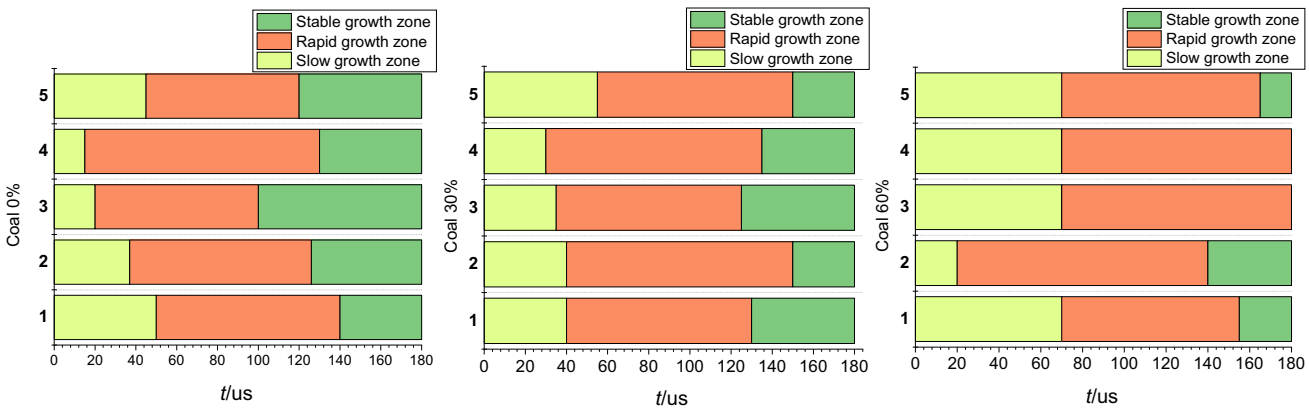

Fig. 5 Effect of moisture content of coal samples on transformation of stress properties

As the moisture increases from 0% to 30%, the coal particles are gradually wetted by the moisture. Owing to the gradual agglomeration of the wet coal particles, the cohesion between the pore and fissure structures of the coal mass is enhanced, thereby improving the compressive strength of the briquette to a certain extent. When the moisture content of the coal sample is 60%, the pulverized coal particles are gradually surrounded by moisture. As a result, the cohesion is reduced, and the compressive strength of the coal sample may also be reduced. The above impact compression test shows that the compressive strength of coal samples and the overall proportion of different stages are closely related to moisture. In addition, the ratio of activated carbon to pulverized coal has an important influence on the compressive stress, expansion stress and failure stress of coal samples. The greater the ratio of activated carbon to pulverized coal, the more obvious the transformation of the three stresses, as shown in Fig. 5.

Figure 6 shows the impact failure modes of the coal samples with different moisture contents. It can be clearly seen that when the water content is 0%, 30% and 60%, the Nos. 1–5 coal samples all undergo longitudinal compression failure. And from one end of the incident rod, obvious cracks are generated, until the coal sample is completely destroyed. However, when the moisture content of the coal sample increases, the coal sample is impacted by the incident rod, the middle part of the coal sample begins to expand and deform, and one end of the transmission rod also begins to break. The failure mode changes from damage on one side to damage on both sides.

According to the theoretical analysis of microscopic coal mass water soaking softening, when the amount of moisture added to the dry coal particles reaches a reasonable range, the pulverized coal particles and water combine with each other, thereby promoting the agglomeration of coal particles and increasing the overall cohesive force of the coal (Jiang et al. 2016). When pulverized coal particles are subjected to an impact force, greater force is required to separate the particles. The above is the process of converting the macroscopic impact force of the coal mass into the microscopic separation force of the pulverized coal particles. When the amount of water added to dry coal particles exceeds a reasonable range, the volume of the liquid bridge formed between particles increases. However, the volume of the pore structure between the particles is ultimately limited, and thus more moisture will gradually wrap around the particles, allowing the liquid to penetrate. This process reduces the cohesive force between particles. If the coal sample is subjected to an external impact load, instability and damage are more likely to occur. From the energy consumption analysis of the coal samples with different moisture contents, the microscopic liquid bridging force between particles and water can reflect the macroscopic failure mode of the coal samples.

Through theoretical and experimental analysis, the water softening degree of the coal sample is affected by the composition of the coal sample, especially the components of cement and activated carbon in the coal sample. The greater the proportion of the cement component in the coal sample, the more obvious the softening degree of the coal sample, and the smaller the influence of the activated carbon component. Therefore, the microscopic effect of moisture on coal samples can be reflected from the macroscopic point of the experiment.

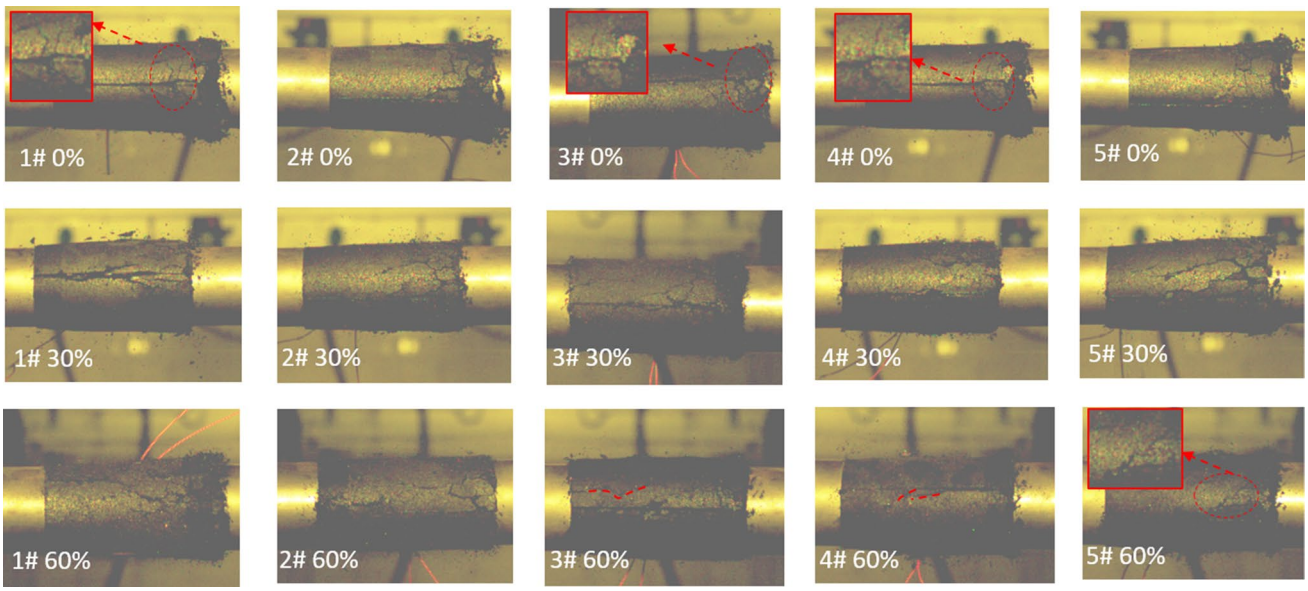

Fig. 6 Effect of coal sample immersion on transformation of stress properties

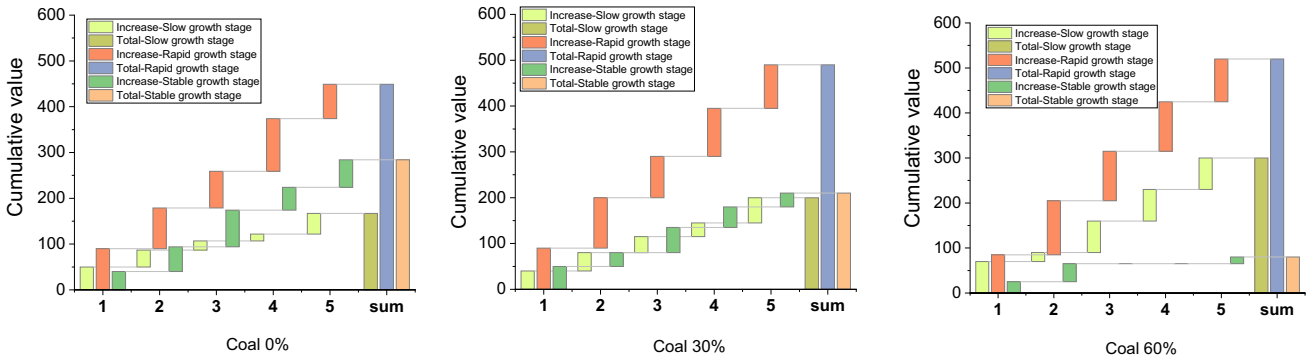

Fig. 7 Strain rate variation of three coal samples with different moisture contents

Figure 7 shows the strain rate variation of the coal samples with three different moisture contents and five compositions. In Fig. 7, the strain rates of the Nos. 1 and 5 coal samples are used as reference values, and there is no obvious change and uniformity change in the rapid growth stage. From the overall analysis, with the increase of the water content, the slow growth stage increases while the stable growth stage decreases. Especially when the water content of the coal sample is 60%, there is no stable growth stage for the Nos. 3 and 4 coal samples. From the analysis of coal sample composition, the proportions of coal particles and sand in the Nos. 1 and 5 coal samples are the same, but the cement component gradually increases. Therefore, when the moisture content of the coal sample is high, the deformation of the coal sample is affected.

From the energy analysis of the coal sample, the energy change of the coal sample during the entire destruction process is obvious, which mostly occurs after 50 μs. In the early stage, there is a process of energy accumulation. After the coal sample is destroyed, the energy decreases rapidly. This experiment shows that reasonable moisture can promote the agglomeration of dry coal particles. When the moisture exceeds certain content, the agglomeration effect of moisture on coal particles is weakened.

In summary, the composition ratios of the Nos. 3 and 4 coal samples are not suitable for water immersion experiments of high water content coal. In the case of three water contents, the slow growth stage of the No. 1 coal sample is relatively long, and thus the No. 1 coal sample is used for the coal immersion softening experiment because of its optimal composition ratio.

4 Conclusions

In this paper, the SHPB experiments were carried out on five coal samples with three different moisture contents, and the dynamic characteristics and energy dissipation of water-immersed coal with different compositions and water contents were analyzed. After analysis and discussion, the following conclusions are drawn:

(1) When the moisture content of the coal sample is 0%, 30%, 60%, the stress, strain rate, and energy dissipation of the coal sample first increase and then decrease with time, while the strain of the coal sample almost increases all the time with slow growth stages and rapid growth stages.
(2) When the water content of the coal sample increases from 30% to 60%, the stress "plateau" of the coal sample becomes more obvious, the rate of stress increase decreases, the compressive stress stage increases, and the expansion stress stage decreases.
(3) The increase of water content of coal will affect the impact deformation and failure mode of coal. When the water content is 0% and 30%, the coal sample undergoes compression deformation and destruction from one end of the incident rod; but when the water content is 60%, the middle part of the coal sample is expanded and deformed.
(4) The optimal coal composition ratio for this impact experiment of coal immersion softening is: "No. 425 Ordinary Portland Cement: 4%, River sand (20–40 mesh): 3.5%, Water: 8.25%, Granular activated carbon Φ2.6 mm × 5.6 mm: 0.88%, Coal powder (20–40, 40–80 mesh ratio 1:1): 83.37%".

Author contributions GW and ZL interpreted the results and wrote the manuscript. JL, HZ and HL conceived and designed the experiments and theoretical models; HS and JL performed the experiments. All authors read and approved the final manuscript.

Funding This research was funded by the National Natural Science Foundation of China (51974176, 51934004), Shandong

Province Natural Science Foundation of Outstanding Youth Fund (ZR2020JQ22), Shandong Province Colleges and Universities Youth Innovation and Technology Support Program (2019KJH006), and Taishan Scholars Project (TS20190935).

Declarations

Competing interests We declare that we have no financial and personal relationships with other people or organizations that can inappropriately influence our work, there is no professional or other personal interest of any nature or kind in any product, service and/or company that could be construed as influencing the position presented in, or the review of, the manuscript entitled.

References

Ai D, Zhao Y, Wang Q, Li C (2020) Crack propagation and dynamic properties of coal under SHPB impact loading: experimental investigation and numerical simulation. Theor Appl Fract Mec 105:102393. https://doi.org/10.1016/j.tafmec.2019.102393

Al-Salloum Y, Almusallam T, Ibrahim SM, Abbas H, Alsayed S (2015) Rate dependent behavior and modeling of concrete based on SHPB experiments. Cem Concr Compos 55:34–44. https://doi.org/10.1016/j.cemconcomp.2014.07.011

Bariani PF, Berti G, Corazza S (2011) Enhancing performances of SHPB for determination of flow curves. CIRP Ann 50(1):153–156. https://doi.org/10.1016/S0007-8506(07)62093-9

Bo-bo LI, Zhong-hui WA, Chong-hong RE, Yao ZH, Jiang XU (2021) Mechanical properties and damage constitutive model of coal under the coupled hydro-mechanical effect. Rock Soil Mech 42(2):315–332

Butt U, Xue P (2014) Determination of the wave propagation coefficient of viscoelastic SHPB: Significance for characterization of cellular materials. Int J Impact Eng 74:83–91. https://doi.org/10.1016/j.ijimpeng.2013.11.010

Chengwu LI, Beijing XIE, Wei Y, Zhuang X (2012) Coal impact damage SHPB testing signal de-noising based on HHT method. J China Coal Soc 37(11):1796–1802

Chengwu L, Qifei W, Pingyang L (2016) Study on electromagnetic radiation and mechanical characteristics of coal during an SHPB test. J Geophys Eng 13:391. https://doi.org/10.1088/1742-2132/13/3/391

Daryadel SS, Ray C, Pandya T, Mantena PR (2015) Energy absorption of pultruded hybrid glass/graphite epoxy composites under high strain-rate SHPB compression loading. Mater Sci Appl 6:511–518

Denggao J, Zu'ne W, Lijuan Z (2005) The examination study of the size-composition of the fine-coal briquetting. J China Coal Soc 1(30):100–103

Doner S, Nayak S, Senol K, Shukla A, Krishnan NA, Yilmazcoban IK, Das S (2019) Dynamic compressive behavior of metallic particulate-reinforced cementitious composites: SHPB experiments and numerical simulations. Constr Build Mater 227:116668. https://doi.org/10.1016/j.conbuildmat.2019.08.049

Erguler ZA, Ulusay R (2009) Water-induced variations in mechanical properties of clay-bearing rocks. Int J Rock Mech Min 46:355–370. https://doi.org/10.1016/j.ijrmms.2008.07.002

Fan L, Ma L, Yihe Yu, Wang S, Yujun Xu (2019) Water-conserving mining influencing factors identification and weight determination in Northwest China. Int J Coal Sci Technol 6(1):95–101. https://doi.org/10.1007/s40789-018-0233-2

Fan C, Li S, Elsworth D, Han J, Yang Z (2020) Experimental investigation on dynamic strength and energy dissipation characteristics of gas outburst-prone coal. Energy Sci Eng 8:1015–1028. https://doi.org/10.1002/ese3.565

Feng J, Wang E, Chen L, Li X, Xu Z, Li G (2016) Experimental study of the stress effect on attenuation of normally incident P-wave through coal. J Appl Geophys 132:25–32. https://doi.org/10.1016/j.jappgeo.2016.07.001

Feng J, Wang E, Huang Q, Ding H, Zhang X (2020) Experimental and numerical study of failure behavior and mechanism of coal under dynamic compressive loads. Int J Min Sci Technol 30(5):613–621. https://doi.org/10.1016/j.ijmst.2020.06.004

Hao X, Du W, Zhao Y, Sun Z, Zhang Q, Wang S, Qiao H (2020) Dynamic tensile behaviour and crack propagation of coal under coupled static-dynamic loading. Int J Min Sci Technol 30(5):659–668. https://doi.org/10.1016/j.ijmst.2020.06.007

Jacquelin D, Brizard S, Ronel E (2017) Estimating measurement uncertainty on stress-strain curves from SHPB. Exp Mech 57:735–742. https://doi.org/10.1007/s11340-017-0260-8

Jiang CB, Duan MK, Yin GZ, Wu GP, Yu H (2016) Loading-unloading experiments of coal containing gas under the condition of different moisture contents. J China Coal Soc 41(9):2230–2237

Kim EH, de Oliveira DB (2015) The effects of water saturation on dynamic mechanical properties in red and buff sandstones having different porosities studied with Split Hopkinson Pressure bar (SHPB). Appl Mech Mater 752–753:784–789. https://doi.org/10.4028/www.scientific.net/AMM.752-753.784

Kim BH, Walton G, Larson MK, Berry S (2021) Investigation of the anisotropic confinement-dependent brittleness of a Utah coal. Int J Coal Sci Technol 8(2):274–290. https://doi.org/10.1007/s40789-020-00364-7

Kong X, Wang E, Li S, Lin H, Zhang Z, Ju Y (2020) Dynamic mechanical characteristics and fracture mechanism of gas-bearing coal based on SHPB experiments. Theor Appl Fract Mech 105:102395. https://doi.org/10.1016/j.tafmec.2019.102395

Kong X, Li S, Wang E, Ji P, Wang X, Shuang H, Zhou Y (2021a) Dynamics behaviour of gas-bearing coal subjected to SHPB tests. Compos Struct 256:113088. https://doi.org/10.1016/j.compstruct.2020.113088

Kong X, Li S, Wang E, Wang X, Zhou Y, Ji P, Shuang H, Li S, Wei Z (2021b) Experimental and numerical investigations on dynamic mechanical responses and failure process of gas-bearing coal under impact load. Soil Dyn Earthq Eng 142:106579. https://doi.org/10.1016/j.soildyn.2021.106579

Lama RD, Bodziony J (1998) Management of outburst in underground coal mines. Int J Coal Geol 35:83–115

Larbi G, Mostapha T, Hocine O, Alaoui AE (2015) A practical note for SHPB test with new algorithms for delimiting pulses. Compos Struct 126:145–158. https://doi.org/10.1016/j.compstruct.2015.02.061

Lin BQ, Zhou SN (1986) Experimental investigation on the deformation law of coal body containing methane. J China Inst Min Technol 3:9–16

Liu XH, Zhang R, Liu JF (2012) Dynamic test study of coal rock under different strain rates. J China Coal Soc 37(9):1528–1534

Liu A, Liu S, Liu P, Wang K (2021) Water sorption on coal: effects of oxygen-containing function groups and pore structure. Int J Coal Sci Technol 8(5):983–1002. https://doi.org/10.1007/s40789-021-00424-6

Majedi MR, Afrazi M, Fakhimi A (2021) A micromechanical model for simulation of rock failure under high strain rate loading. Int J Civ Eng 19(5):501–515. https://doi.org/10.1007/s40999-020-00551-2

Merle R, Zhao H (2006) On the errors associated with the use of large diameter SHPB, correction for radially non-uniform distribution of stress and particle velocity in SHPB testing. Int J Imp Eng 32:1964–1980. https://doi.org/10.1016/j.ijimpeng.2005.06.009

Mishra S, Khetwal A, Chakraborty T (2019) Dynamic characterisation of gneiss. Rock Mech Rock Eng 52(1):61–81. https://doi.org/10.1007/s00603-018-1594-y

Pan Z, Connell LD, Camilleri M, Connelly L (2010) Effects of matrix moisture on gas diffusion and flow in coal. Fuel 89(11):3207–3217. https://doi.org/10.1016/j.fuel.2010.05.038

Perera MSA, Ranjith PG, Peter M (2011) Effects of saturation medium and pressure on strength parameters of latrobe valley brown coal: carbon dioxide, water and nitrogen saturations. Energy 36(12):6941–6947. https://doi.org/10.1016/j.energy.2011.09.026

Qin H, Huang G, Wang WZ (2012) Experimental study of acoustic emission characteristics of coal samples with different moisture contents in process of compression deformation and failure. Chin J Rock Mech Eng 31(6):1115–1120

Roth CC, Gary G, Mohr D (2015) Compact SHPB system for intermediate and high strain rate plasticity and fracture testing of sheet metal. Exp Mech 55:1803–1811. https://doi.org/10.1007/s11340-015-0061-x

Saleh M, Kariem MM, Luzin V, Toppler K, Li H, Ruan D (2018) High strain rate deformation of ARMOX 500T and effects on texture development using neutron diffraction techniques and SHPB testing. Mater Sci Eng A 709:30–39. https://doi.org/10.1016/j.msea.2017.09.022

Tuazon BJ, Bae KO, Lee SH, Shin HS (2014) Integration of a new data acquisition/processing scheme in SHPB test and characterization of the dynamic material properties of high-strength steels using the optional form of Johnson-Cook model. J Mech Sci Technol 28(9):3561–3568. https://doi.org/10.1007/s12206-014-0817-8

Wang B, Li X, Yin T, Ma C, Yin Z, Li Z (2010) Split Hopkinson Pressure Bar (SHPB) experiments on dynamic strength of water-saturated sandstone. Chin J Rock Mech Eng 29(5):1003–1009

Wang K, Jiang YF, Xu C (2018) Mechanical properties and statistical damage model of coal with different moisture contents under uniaxial compression. Chin J Rock Mech Eng 37(5):1070–1079

Wang G, Jiang C, Shen J, Han D, Qin X (2019) Deformation and water transport behaviors study of heterogenous coal using CT-based 3D simulation. Int J Coal Geol 211:103204. https://doi.org/10.1016/j.coal.2019.05.011

Wang G, Li J, Liu Z, Qin X, Yan S (2020) Relationship between wave speed variation and microstructure of coal under wet conditions. Int J Rock Mech Min Sci 126:104203. https://doi.org/10.1016/j.ijrmms.2019.104203

Wolf KH, Bruining H (2007) Modelling the interaction between underground coal fires and their roof rocks. Fuel 86:2761–2777. https://doi.org/10.1016/j.fuel.2007.03.009

Woo SC, Kim TW (2016) High strain-rate failure in carbon/Kevlar hybrid woven composites via a novel SHPB-AE coupled test. Compos Part B 97:317–328. https://doi.org/10.1016/j.compositesb.2016.04.084

Xiao X, Jin C, Ding X, Pan Y (2018) Experimental study on rock burst tendency of coal with different moisture content based on acoustic emission time-frequency signals. J China Coal Soc 43(4):931–938

Xu J, Liu D, Peng S, Wu X, Lu Q (2010) Experimental research on influence of particle diameter. Chin J Rock Mech Eng 29(6):1231–1237

Yin G, Jiang C, Xu J, Guo L, Peng S, Li W (2012) An experimental study on the effects of water content on coalbed gas permeability in ground stress fields. Transp Porous Med. https://doi.org/10.1007/s11242-012-9990-3

Yin Z, Chen W, Hao H, Chang J, Zhao G, Chen Z, Peng K (2020) Dynamic compressive test of gas-containing coal using a modified split Hopkinson pressure bar system. Rock Mech Rock Eng 53(2):815–829. https://doi.org/10.1007/s00603-019-01955-w

Yu MG, Chao JK, Chu TX, Teng F, Li P (2017) Experimental study on permeability parameter evolution of pressure-bear broken coal. J China Coal Soc 42(4):916–22

Zhang Z, Zhao D, Chen Y (2020) Isothermal adsorption and swelling deformation characteristics of soft coal under different moisture content. J China Coal Soc 45(11):3817–3824

Zhao Y, Zhao GF, Jiang Y, Elsworth D, Huang Y (2014) Effects of bedding on the dynamic indirect tensile strength of coal: laboratory experiments and numerical simulation. Int J Coal Geol 132:81–93. https://doi.org/10.1016/j.coal.2014.08.007

Zhao D, Li X, Tang Y, Wang W, Feng Z (2020) Study of gas adsorption characteristics influenced by moisture content, different coal particle sizes, and gas pressures. Arab J Geosci 13(15):1–14. https://doi.org/10.1007/s12517-020-05748-2

Zhu J, Hu S, Wang L (2009) An analysis of stress uniformity for concrete-like specimens during SHPB tests. Int J Impact Eng 36(1):61–72. https://doi.org/10.1016/j.ijimpeng.2008.04.007